Chapter 2

Principle of Prestack Migration Velocity Analysis

The philosophy behind any velocity analysis method is summarized by this simple argument:

Given: Operation A depends on property p.
Corollary: Property p can be deduced from the effect of operation A.

Seen in this light, normal moveout is just one possible operation that can be used to deduce the desired property (velocity). This thesis makes use of another operation, migration, as the velocity analysis tool. The difference between NMO and migration is that NMO is a time shift while migration is both a time and a space shift. It should be observed that we must retain offset and migrate the unstacked data because, it is the relation between traveltime and offset that is governed by the velocity and this relation is what we use for velocity analysis.

2.1 A VELOCITY ANALYSIS PRINCIPLE

The principle behind the prestack migration velocity analysis of this thesis can be stated as follows:

> After migration with the correct velocity model, images in a common-receiver gather (CRG) are aligned horizontally, regardless of structure.

A common-receiver gather is a gather that has the same receiver coordinate as shown in Figure 2.1. It represents a fixed surface location. Because the CRG is examined after

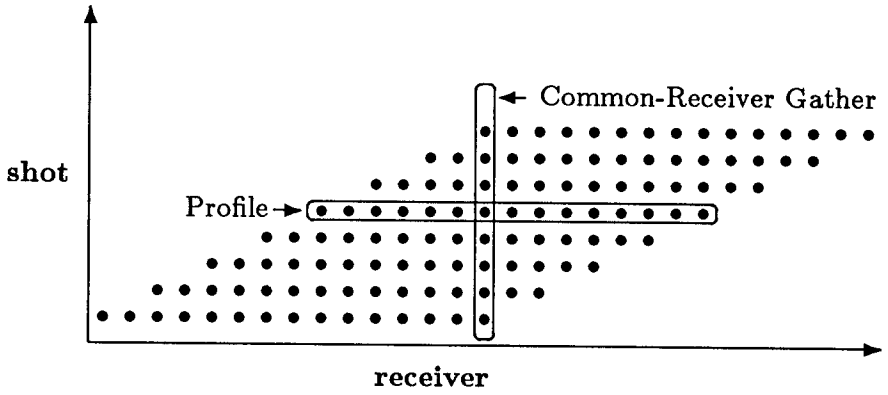

FIG. 2.1. A stacking chart showing a common-receiver gather (CRG).

migration, I will refer to it as post-migration CRG.

The interpretation of this principle is intuitive. When imaged correctly, the image of the subsurface under a surface location should be at the same depth, regardless of the source position. The analogue concept in a Common Midpoint Gather (CMP) is the alignment of reflections after NMO with the correct (stacking) velocity. There is, however, an important difference between the post-migration CRG and the NMO'ed CMP gather. The difference is that the alignment of images in a CRG takes place *regardless* of structure; it depends only on the velocity. On the other hand, the alignment of reflections in a CMP gather depends on the dip of the reflector; higher velocities are needed for higher dips.

I will illustrate this velocity analysis principle by migrating the synthetic profile shown in Figure 2.2. In Figure 2.3a the profile is migrated with the velocity of the medium and in Figure 2.3b it is migrated with a lower velocity.

We know that the velocity used in Figure 2.3b is wrong (too low in this case) because we did not obtain the image we were expecting, namely a flat horizontal reflector like the one in Figure 2.3a. However, we normally do not know the structure and therefore cannot determine whether the velocity used in migration is or is not correct. A common-receiver gather, on the other hand, shows the image of the subsurface under one surface location. Therefore, after migration this image should be at the same depth for all source offsets. Figure 2.4 shows a post-migration CRG. This CRG is obtained from 40 profiles, of which

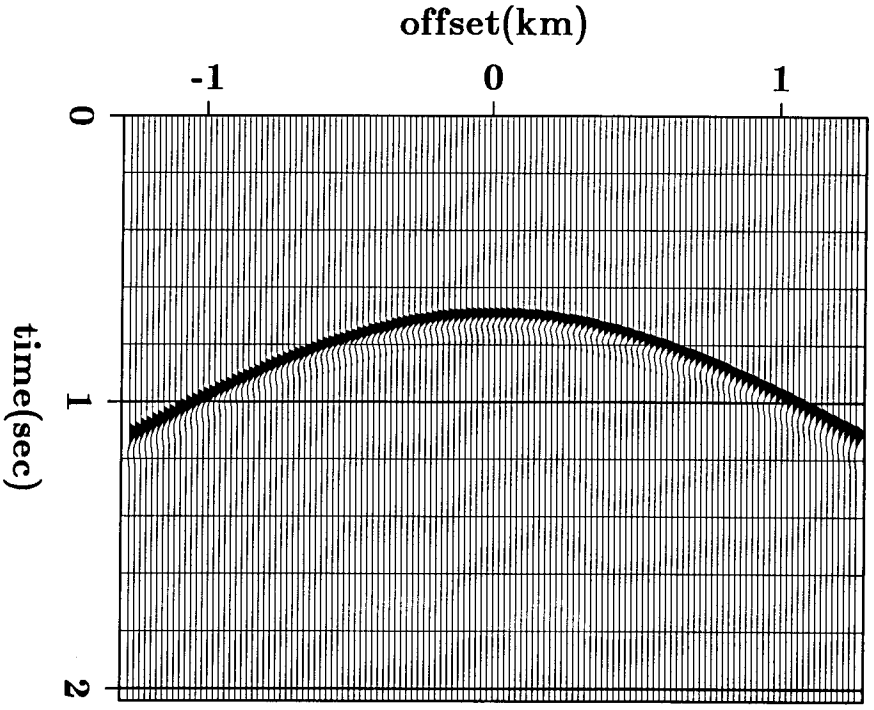

FIG. 2.2. A synthetic profile for a horizontal reflector. A constant velocity of 1.5 km/sec was used in the modeling.

the profile in Figure 2.3 is representative. In this case, where the reflector is horizontal, a common-shot gather and a common-receiver gather are similar, except for the number of traces in each gather.

In Figure 2.4, where the migration velocity is lower than the velocity of the medium, the image is curved upward. As shown later, if the migration velocity had been higher than the velocity of the medium the image would be curved downward.

Note that, as mentioned previously, the alignment in a CRG is independent of structure. Figures 2.5 and 2.6 illustrate this fact. Figure 2.5 shows a migrated synthetic profile and some CRG's for a dipping reflector when the migration velocity is the same as the velocity of the medium; Figure 2.6 shows the same profile and the CRG's migrated with a velocity that is lower than the velocity of the medium. Note the alignment of the image when the migration velocity was the same as the velocity of the medium in spite of the dip of the reflector. Had NMO been used instead of migration, the image would be aligned horizontally after using a velocity that is higher than the velocity of the medium by a

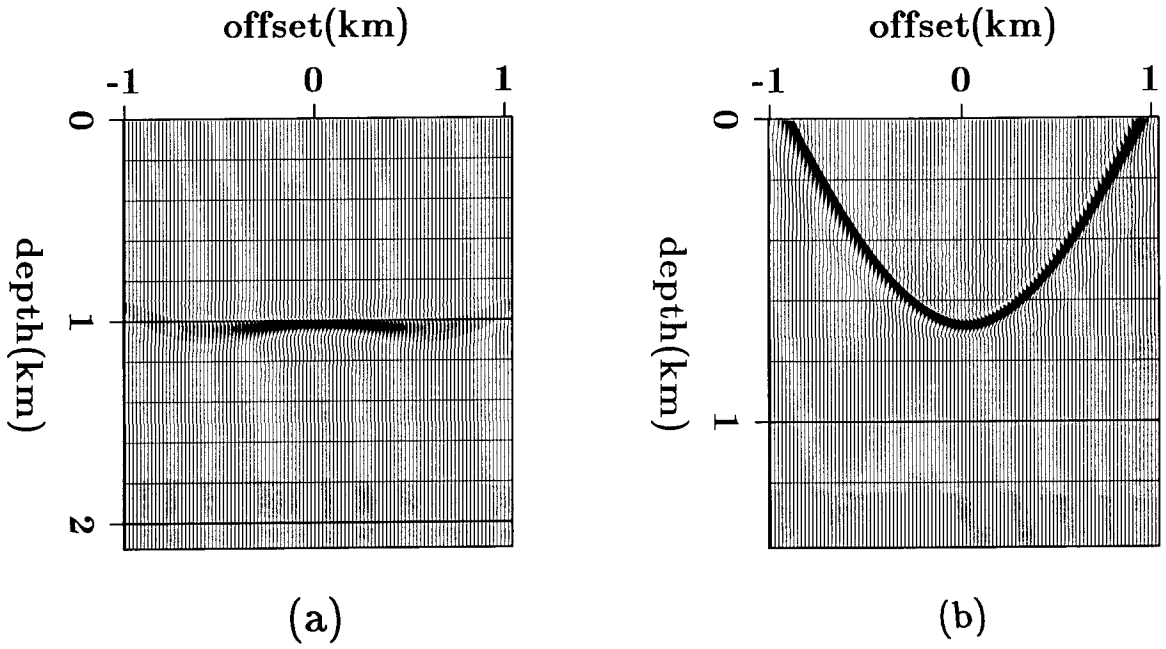

FIG. 2.3. The profile of Figure 2.2 after migration. (a) with the correct velocity (1.5 km/sec). (b) with a low velocity (1 km/sec). Note that at the edge of the illuminated area truncation effects cause some curvature even when the correct velocity is used. These edge effects are attenuated by stacking.

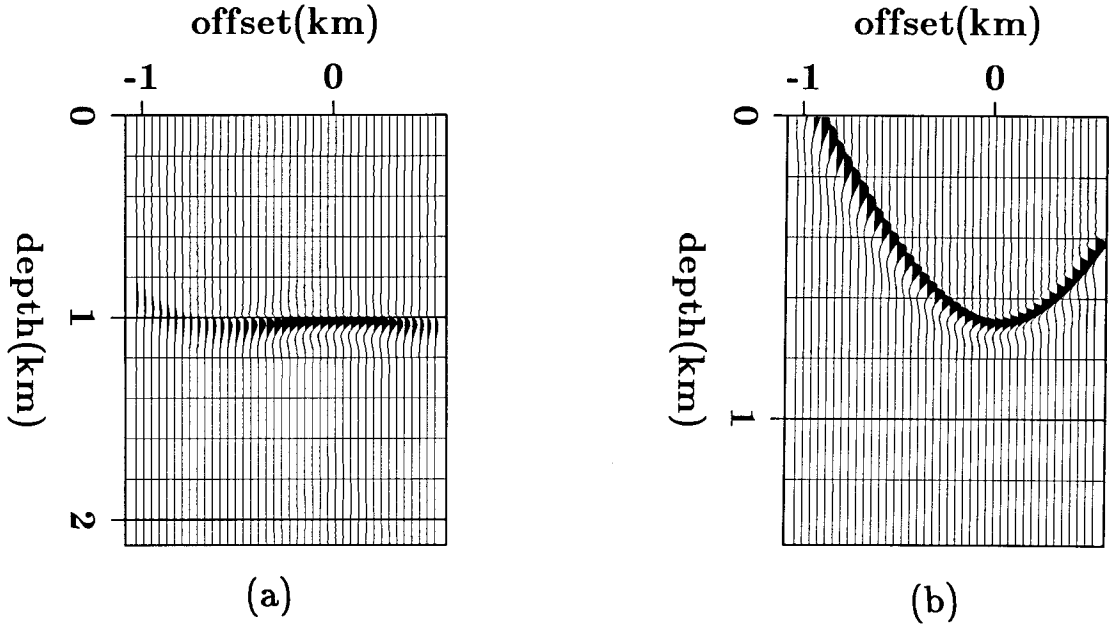

FIG. 2.4. A CRG from migrated profiles like the one in Figure 2.3. (a) with the correct velocity (1.5 km/sec). (b) with a low velocity (1 km/sec).

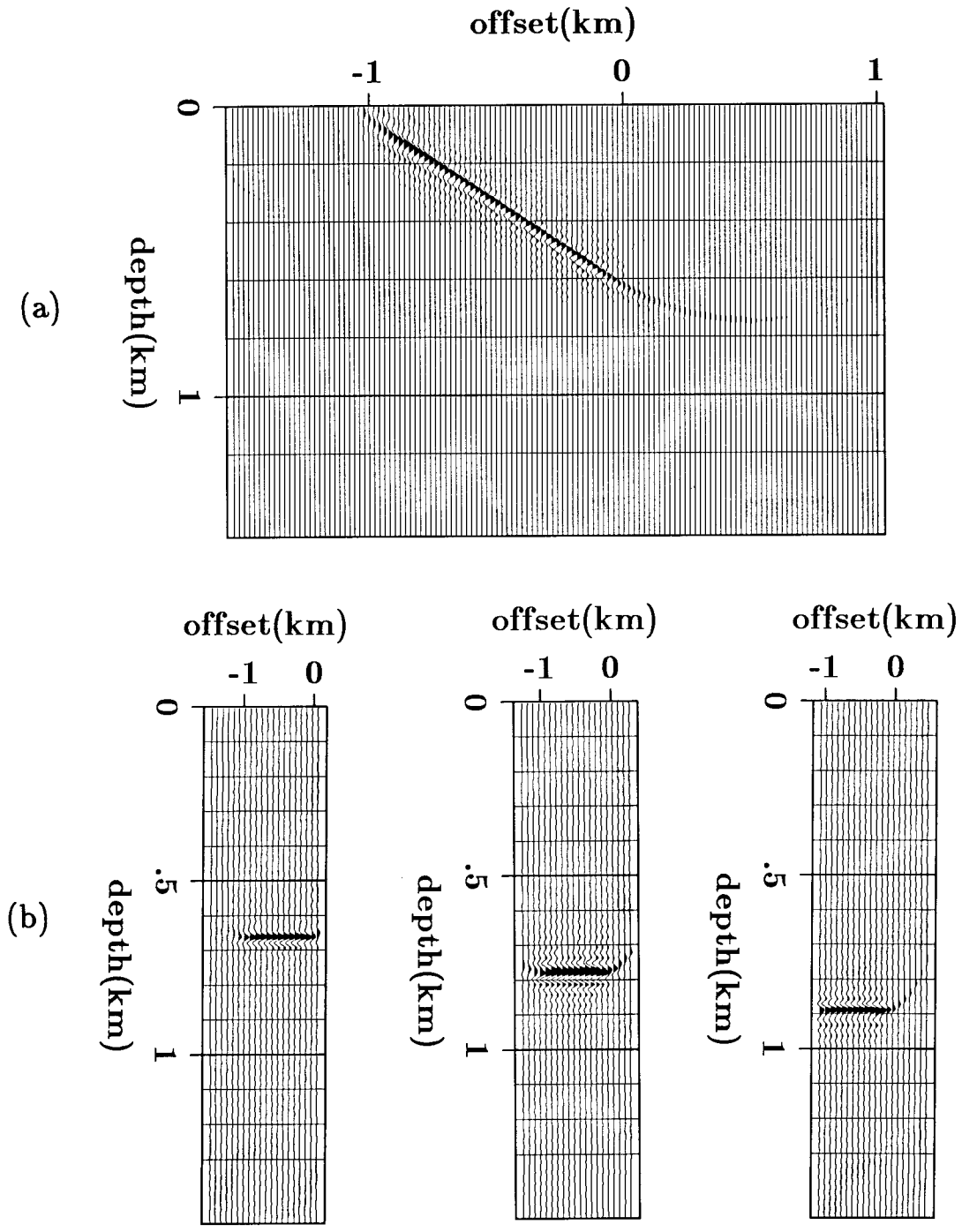

FIG. 2.5. (a) A migrated profile for a dipping-reflector model. The dip angle is 30° and the velocity used in migration (1.5 km/sec) is the same as the velocity of the medium. (b) Some CRG's from the migrated profiles. Note that the depth of the image varies between CRG's because the reflector is dipping.

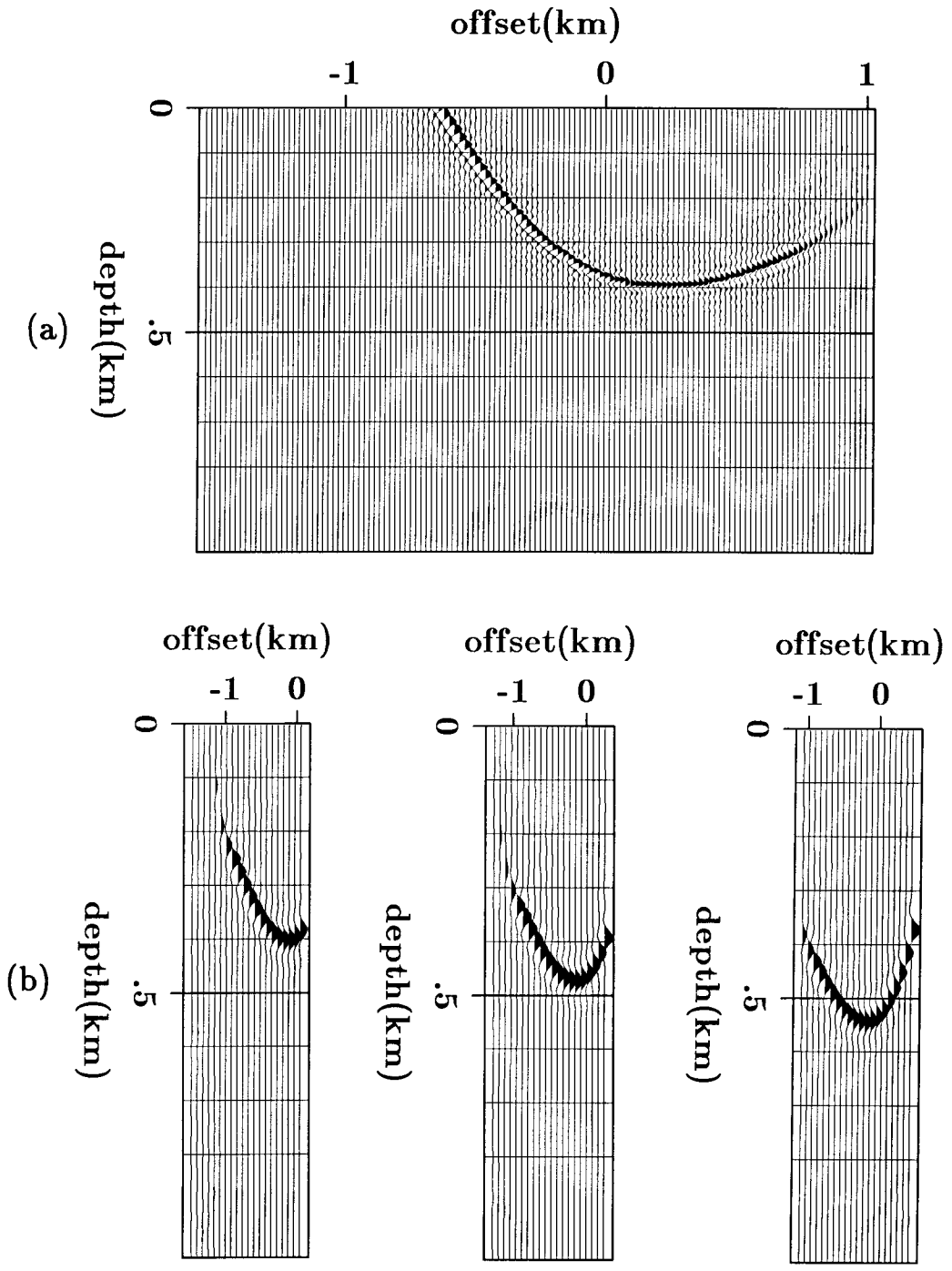

FIG. 2.6. (a) A migrated profile for a dipping-reflector model. The dip angle is 30° and the velocity used in migration (1 km/sec) is lower than the velocity of the medium (1.5 km/sec). (b) Some CRG's from the migrated profiles.

factor equal to the secant of the dip angle (Levin, 1971). Alternatively, DMO would need to have been applied. As noted earlier, DMO is not adequate if the velocity varies laterally.

The velocity analysis principle stated earlier needs some explanation. First, it is important to note that a CRG is examined after *all* the data has been migrated. The velocity analysis principle does not apply to a singly migrating CRG, because the migrated image under a CRG does not necessarily come from the receiver at that surface location. Therefore, we need first to have *all* CRG's migrated. Second, in a CRG, we have images that come from different sources which may have different wavelet shapes. Because these sources are at different offsets, there are also amplitude variations among these images. This variation in phase and amplitude is ignored in the velocity analysis principle, which addresses kinematics only. Third, note that the alignment of images occurs at *all depths* if the true interval velocity is used in migration.

In the formulation that follows, slowness (the reciprocal of velocity) is used instead of velocity itself. Using slowness makes the analysis simpler because travel time is linear with slowness rather than velocity. Velocity and slowness will sometimes be used interchangeably when either will serve the purpose.

If the image of one reflector is aligned while the images of reflectors above it are not aligned, all we can tell is that the *average* slowness above the lower reflector is correct, while the interval slowness is not. Figures 2.7 and 2.8 illustrate this point. In both figures, the lower reflector appears flat in the post-migration CRG even though the interval slownesses above that reflector are different in the two cases. If the upper reflector did not exist, we would have no way of telling which velocity model is the correct one; there is no unique model that produces horizontally-aligned images. However, the upper reflector provides a constraint because we seek to align both images. In practice, the distance between reflectors is small enough to provide enough constraints on the velocity.

From the point of view of reciprocity , sources and receivers are interchangeable if they are downward continued in the same way. A common-source gather and a common-receiver gather are, therefore, equivalent. This argument prompts two questions. First, why don't we migrate CRG's instead of profiles? Second, why do we look at post-migration CRG's rather than migrated profiles? The first question was answered in section 1.4, where profiles migration was discussed. The important reason here is that spatial sampling is better in the receiver axis than it is in the source axis. The second question is answered by the velocity analysis principle mentioned above. A migrated profile has an image of an

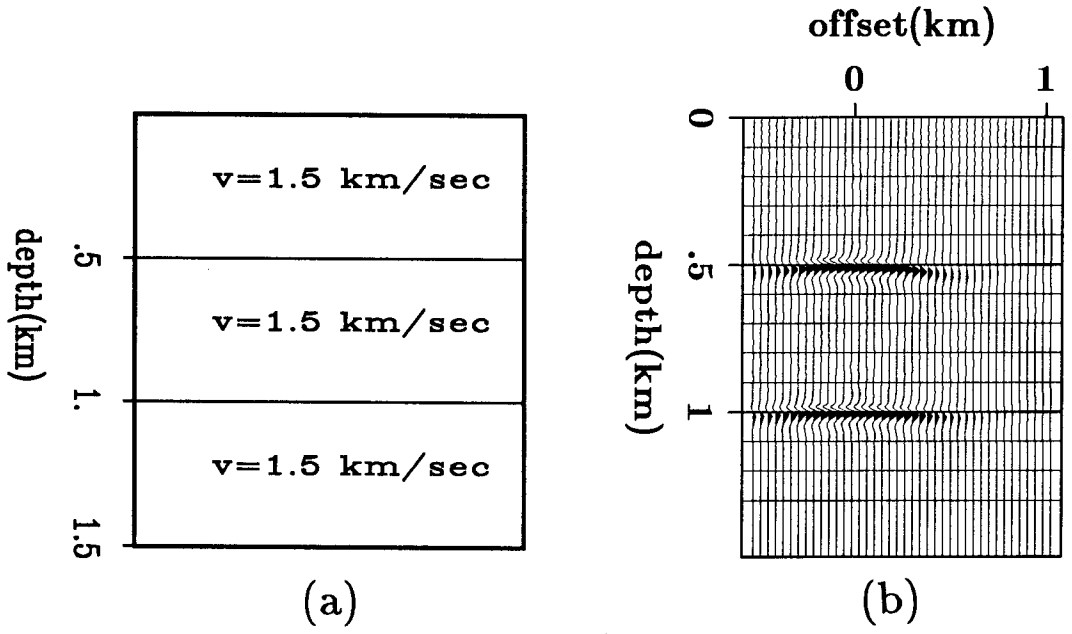

FIG. 2.7. (a) A layered model. (b) A post-migration CRG for the layered model in (a). The images of both reflectors are aligned horizontally because the velocity used in migration is the same as the velocity of the model.

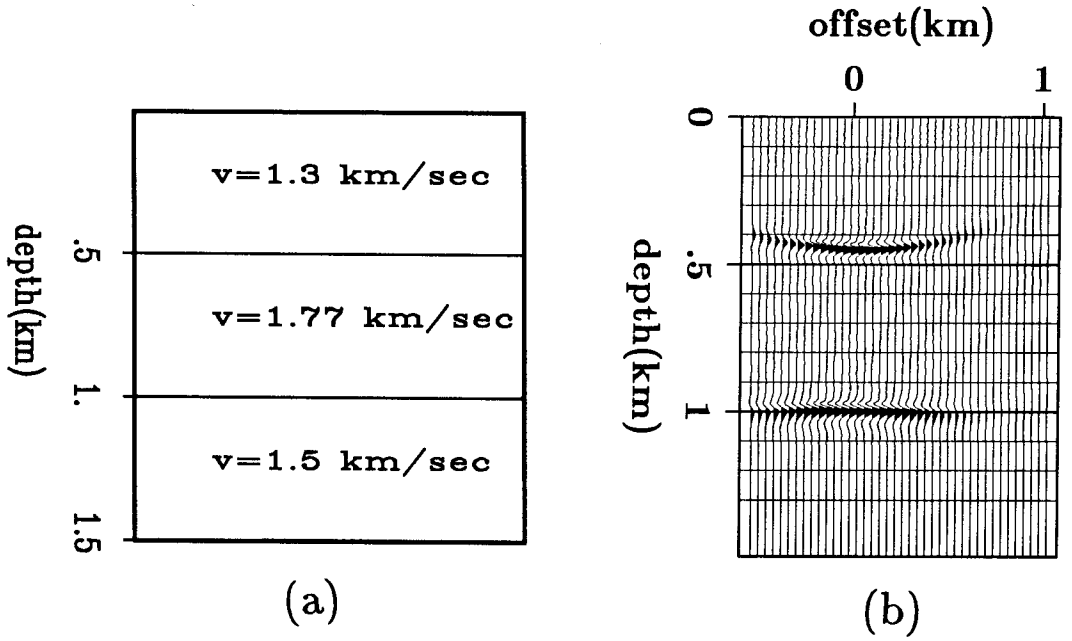

FIG. 2.8. (a) A layered model. The average slowness to the lower reflector is the same as that in Figure 2.7a, but the interval slownesses are different. (b) A post-migration CRG obtained by migrating the data using the model in (a). Note that the lower reflector appears horizontally-aligned as in Figure 2.7b, but that the upper reflector is not aligned because the velocity used in migration is too low for the first layer (or slowness is too high).

area, while a post-migration CRG has the image under *one* surface location. The image in the post-migration CRG is obtained after all CRG's have been migrated or, alternatively, as argued previously, after all profiles have been migrated.

We are therefore able to make a qualitative comparison between CRG's to determine which one was migrated with a velocity that is the closest to the velocity of the medium. From the type of curvature (upward or downward) we are also able to tell whether the velocity used in migration is higher or lower than the velocity of the medium. Later in this chapter, I will use this idea to estimate the error in average velocities (or rather the average slowness). In the next chapter I will estimate interval velocities (or interval slownesses). First, I will discuss what possible velocity analysis methods can be devised using this idea.

2.2 PRESTACK MIGRATION VELOCITY ANALYSIS METHODS

Since images are aligned horizontally in a post-migration CRG that is migrated with the correct velocity model, then stacking along the shot axis will produce the biggest signal when the velocity is correct. Therefore, one approach to prestack migration velocity analysis is to scan the velocity space and check which velocity model produces the biggest signal at all depths. This "Monte Carlo"-type searching is too expensive, because migration is not a trivially cheap process that can be repeated a large number of times. Even an annealing approach similar to the one proposed by Rothman (1985) for the statics problem is too expensive for migration velocity analysis.

Yilmaz and Chambers (1984) proposed one method of prestack migration velocity analysis Their method was implemented in the Fourier domain where velocity cannot vary laterally. The principle they used is that the image in the (t, τ) space should fall on the line $t = \tau$ if the velocity is correct, where t is the traveltime and τ is the traveltime depth. The correction to the velocity model if events do not fall on the line $t = \tau$ remains to be found.

We can follow conventional velocity analysis and do constant-velocity migration and stacking. This constant velocity migration and stacking results in a panel like the one in Figure 2.9a which is similar to the conventional NMO-stacking velocity panel in Figure 2.9b. From these constant velocities, an interval-velocity model is obtained. This scheme resembles Toldi's method of velocity analysis from NMO-stacked data (Toldi, 1985). In this scheme we optimize an objective function that measures the strength of the signal when stacked over the shot axis. A similar approach is taken by Fowler (1985b)

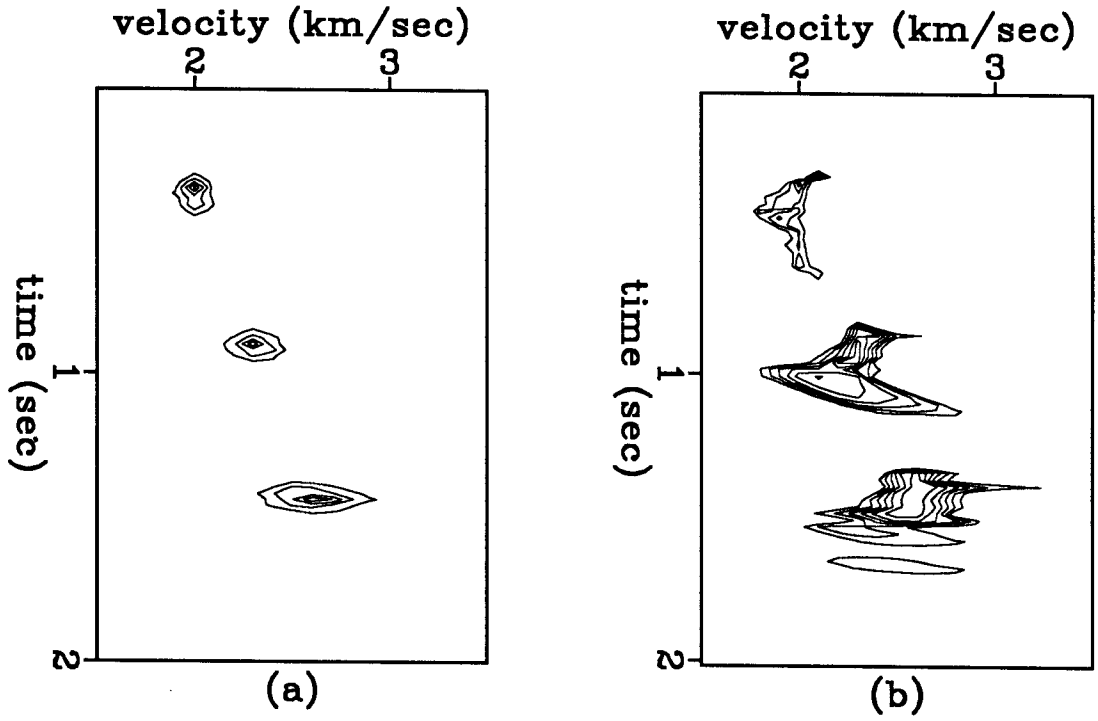

FIG. 2.9. (a) Velocity panel produced by constant-velocity prestack migration and stacking. (b) Velocity panel produced by NMO and stacking.

who implements it in the offset-midpoint (h, y) space. Whether the migration is implemented in the (s, g) space or the (h, y) space, the velocity analysis principle mentioned earlier remains unchanged.

When we are searching for a velocity model from constant velocity stacks, the velocities have to be close enough to allow interpolation. Fowler (1985a) finds the necessary velocity sampling for NMO and for post-stack migration. The necessary sampling for prestack-migration velocity stacks can be found by combining the limits on both NMO and post stack migration. In Appendix B, I derive a formula for velocity sampling that is based solely on prestack migration.

Instead of searching for a velocity model from constant-velocity stacks, an iterative approach is taken this thesis. That is, after migration with an initial velocity model, I estimate the error in this velocity model, update the model, migrate again, and so on. If the estimation of the velocity error is within reasonable approximation, we should not need more than a small number of iterations (if it were exact, then we would need only

one iteration!). In the next section, I describe this method in detail.

2.3 ESTIMATING AVERAGE SLOWNESS

In section 2.1, we saw that by examining CRG's we can tell if the velocity used in migration is correct or not. In this section, I estimate the error in the average slowness after migration with a preliminary velocity model. In the next chapter, I discuss obtaining the interval-slowness (or interval-velocity) model from these average slownesses.

To update the velocity model after migration, we need a way of quantifying the deviation of the images in a post-migration CRG from horizontal alignment. That is, we want to estimate by how much we need to change the velocity used in Figure 2.4b so that it looks like Figure 2.4a. We should therefore study what happens if we migrate the data using a velocity that is different from the velocity of the medium. The discussion in section 2.1 showed that the curvature in a post-migration CRG is affected by the error in average slowness. I will therefore first obtain average slownesses, then return to interval slownesses in the next chapter.

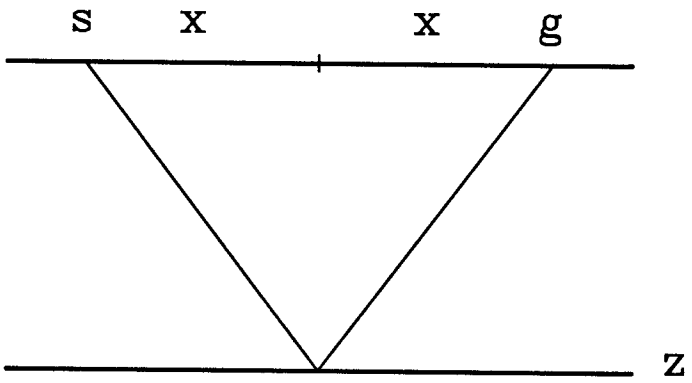

FIG. 2.10. Ray travel path for a flat reflector

2.3.1 Horizontal reflector

I will first discuss the case of a horizontal reflector as shown in Figure 2.10. Let the depth to the reflector be z, the average slowness of the medium to the reflector be $\bar{w}$, and the

recorded traveltime t. If we let the half offset be x, then the traveltime is given by

$$t = 2\sqrt{x^2 + z^2} \cdot \bar{w} \ , \tag{2.1}$$

where a straight ray path from and to the reflector is assumed. After migration with the slowness of the medium, the image under a surface location will be at the same depth z. If we migrate with an average slowness $\bar{w}_m$ instead of with the slowness of the medium itself, the image under a surface location will be at depth z_m. In this case, the traveltime is given by

$$t = 2\sqrt{x^2 + z_m^2} \cdot \bar{w}_m \ . \tag{2.2}$$

Note that the traveltime, t, is the same in equations (2.1) and (2.2) because it is an observed quantity. The ambiguity occurs between slowness and depth. Eliminating t between equations (2.1) and (2.2), we obtain

$$z_m = \sqrt{\gamma^2 z^2 + (\gamma^2 - 1)x^2} \ , \tag{2.3}$$

where

$$\gamma = \frac{\bar{w}}{\bar{w}_m} \ . \tag{2.4}$$

Equation (2.3) gives a relation between the apparent depth, z_m, and the actual depth, z. They are linked through the parameter γ. Note that they are equal regardless of offset when the slowness used in migration is equal to the slowness of the medium (γ=1). This is the essence of the velocity analysis principle mentioned earlier; the image in a post-migration CRG is aligned horizontally if the velocity model is correct. When γ is not equal to 1, there is both a moveout as a function of offset and a shift at zero offset. At zero offset ($x = 0$), there is the well-known ambiguity between depth and velocity,

$$z_m = \gamma z \ ,$$

or

$$z_m \bar{w}_m = z \bar{w} \ . \tag{2.5}$$

In equation (2.5), we know w_m (the migration slowness that we used) and z_m (the depth given by migration with slowness w_m). We cannot determine both z (the actual depth) and w (the actual slowness), because many combinations of these two quantities may satisfy the relation (2.5). Downward continuation with the wrong slowness is like downward continuation to the wrong depth (Doherty, 1975). This argument explains why velocity analysis cannot be done by zero-offset migration.

Using traveltime instead of depth makes the interpretation of (2.5) easier. Recasting equation (2.3) in time,

$$\tau_m = \sqrt{\tau^2 + (\gamma^2 - 1)x^2\bar{w}_m^2}\ , \tag{2.6}$$

where $\tau = z\bar{w}$ and $\tau_m = z_m\bar{w}_m$.

Note that in equation (2.6), we have $\tau_m = \tau$ at zero offset regardless of migration slowness; error in slowness is manifested only in non-zero offsets. Also, as expected, $\tau_m = \tau$ for all offsets when $\gamma = 1$. If the slowness used in migration is too high ($\gamma < 1$), the image in the post-migration CRG will be curved upward as in Figure 2.4b,. If the slowness used in migration is too low ($\gamma > 1$), the image will be curved downward.

The curvature in a post-migration CRG will vary from depth to depth, depending on the velocity error at each depth. Therefore, the parameter γ is not a constant for a CRG but rather a function of depth, $\gamma(z)$ or $\gamma(\tau)$. For instance, all the events in the CRG of Figure 2.11a are curved upward, meaning that the slowness used in migration is too high for all depths. In Figure 2.11b, the situation is different; shallow events are curved downward while deep events are curved upward. Because the curvature at any given depth is determined by a single parameter, γ, there is necessarily a spatial smearing of the velocity error. The velocity error which affects the image from one source will be projected as though it came from all sources. However, a given location is multiply covered by many rays that pass through it and the velocity error at that location is an average of all velocity errors from all rays. This multiplicity of coverage reduces smearing because if there is an anomaly at a location, all rays will enhance it while if there is no anomaly, not all of them will enhance it.

The curvature (or lack of it) in the CRG's can therefore be used to estimate the error (or lack of it) in the velocity model. This statement makes direct use of the corollary mentioned at the beginning of this chapter. Here, velocity error (the property) is deduced from curvature (the effect) produced by migration (the operation). The curvature and the

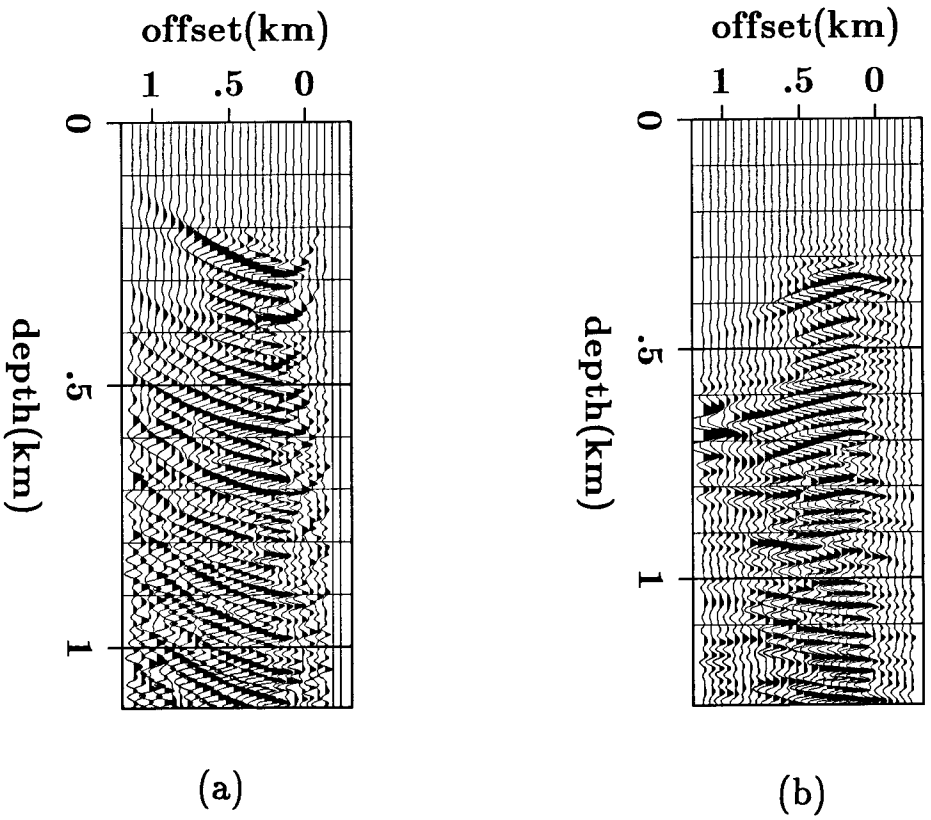

FIG. 2.11. Examples of post-migration CRG's. (a) The slowness used in migration is too high for all depths. All events are curved upward. (b) The slowness used in migration is lower than the slowness of the medium at shallow depths (events curved downward), and is higher than the slowness of the medium for deep events (which are curved upward). The turning point is at about .9 km.

error in average slowness are related via equation (2.6) in which the curvature is determined by the value of γ.

What we need now is a way to measure curvature. I will measure curvature by searching. At each traveltime depth, a curvature is defined by the parameter γ in equation (2.6). The data is then summed along this curved trajectory. The summation is done for a range of γ's and the sum is biggest for that value of γ that matches the curvature. Because some signals may be weaker than others, the sum is normalized. This normalized summation is similar to the normalized summation along a hyperbola using the NMO equation, commonly known as semblance (Taner and Koehler, 1969). If the data in a post-migration

CRG is $p(\tau_m, x)$, then searching for curvature produces the semblance panel $g(\tau, \gamma)$,

$$g(\tau,\gamma) = \frac{\left[\sum_x p\left(\tau_m = \sqrt{\tau^2 + (\gamma^2-1)x^2\bar{w}_m^2}, x\right)\right]^2}{\sum_x \left[p\left(\tau_m = \sqrt{\tau^2 + (\gamma^2-1)x^2\bar{w}_m^2}, x\right)\right]^2} \ . \tag{2.7}$$

The summation path is also given a width, so the summation is also done over a traveltime window. The summation path should be wide enough to include the seismic wavelet.

Equation (2.7) transforms the migrated panel $p(\tau_m, x)$ to the "residual" velocity panel $g(\tau, \gamma)$. Figure 2.12 shows the result of that transformation. In this figure, the data was migrated with a slowness that is the same as the slowness of the medium up to about .35 km and higher than the slowness of the medium beyond that. Visual inspection of the CRG in Figure 2.12a shows that below .35 km, events are curved upward. The semblance panel shows that the values of γ is less than 1 for those events. Had we used the velocity of the medium, all events would lie under $\gamma = 1$ in the semblance panel.

2.3.2 Arbitrary reflector geometry

We would like to have an equation similar to (2.6) but valid for any reflector geometry. Consider the arbitrary reflector geometry shown in Figure 2.13. The traveltime t between the source and receiver is

$$t = \sqrt{a^2 + z^2} \cdot \bar{w} + \sqrt{b^2 + z^2} \cdot \bar{w} \ . \tag{2.8}$$

If $\bar{w}_m$ is used instead of $\bar{w}$,

$$t = \sqrt{a^2 + z_m^2} \cdot \bar{w}_m + \sqrt{b^2 + z_m^2} \cdot \bar{w}_m \ . \tag{2.9}$$

Eliminating t between equations (2.8) and (2.9), we obtain

$$z_m^2 = \frac{\gamma^2}{4} X - \frac{a^2 + b^2}{2} + \frac{(a^2 - b^2)^2}{4\gamma^2 X} \ , \tag{2.10}$$

where

$$X = 2z^2 + a^2 + b^2 + 2\sqrt{z^4 + (a^2 + b^2)z^2 + b^2a^2} \ , \tag{2.11}$$

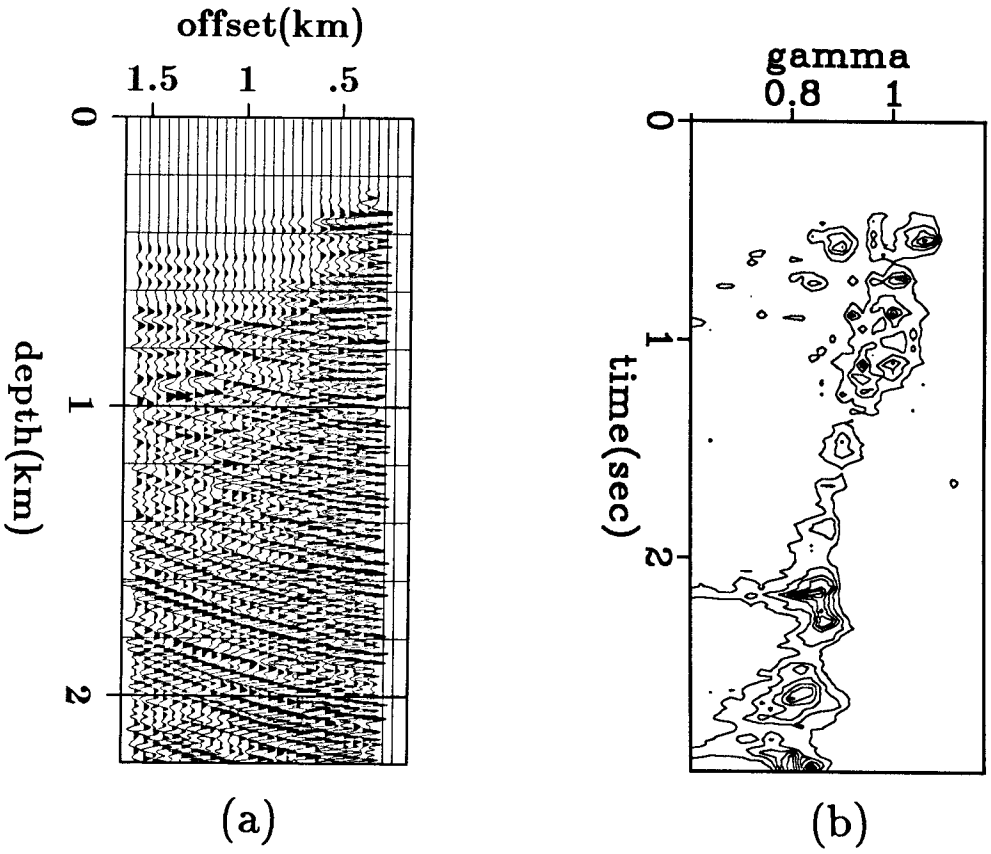

FIG. 2.12. (a) A CRG obtained by migrating with a slowness that is higher than the slowness of the medium. (b) A semblance panel showing the slowness ratio γ vs. traveltime depth.

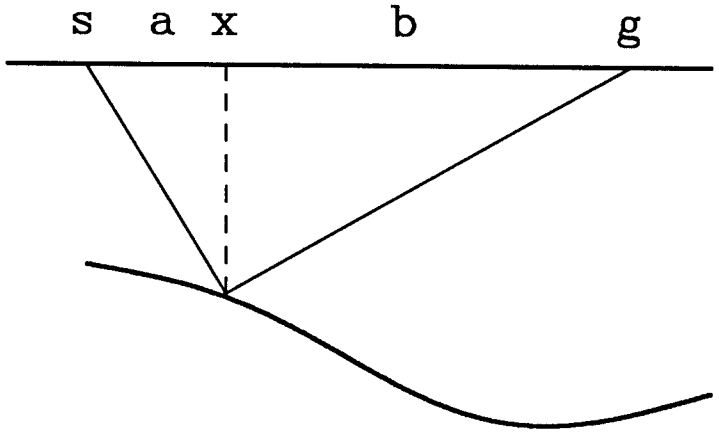

FIG. 2.13. Ray travel path for an arbitrary reflector geometry

and a and b are as shown in Figure 2.13.

Note that equation (2.10) is *structure dependent*; it depends not only on the separation between source and receiver but also on how this separation is partitioned between them into a and b. This partition is in turn dependent on the local dip at the reflection point. It is easily seen that equation (2.10) reduces to equation (2.3) if $a = b$ (a horizontal reflector) and that, as required, $z_m = z$ if $\gamma = 1$. We can further simplify equation (2.10) by noting that the last term is negligible with comparison to the other two, especially when dips are gentle ($a \approx b$). Therefore,

$$z_m^2 \approx \frac{\gamma^2}{4} X - \frac{a^2 + b^2}{2} \,. \tag{2.12}$$

2.3.3 Effect of structure

The structure dependence of equations (2.10) and (2.12) makes it hard to calculate the error in velocity because we need to search not only the source-receiver offset, but also the way it is partitioned between them, namely the local dip at the reflection point.

We should, however, remember that what this method estimates is the *error* in velocity, not the velocity itself. It is acceptable to use an error estimation scheme which is approximate because it will bring us closer to the solution. If the error estimation were exact, then only one iteration would be needed! Moreover, we know that when we have horizontally-aligned images in the post-migration CRG's, then we have *no* error in the velocity and this fact is *structure independent.*

Using equation (2.3) assumes that $a = b$ in equation (2.10). Equation (2.3) (or its equivalent (2.6)) ignores the effect of structure. Ignoring the structure can be justified if we can show that the difference between equations (2.3) and (2.10) diminishes as we become closer to the solution. Let's compute the difference in apparent depth (z_m) given by the two equations. Let the depth given by equation (2.10) be z_1 and that given by equation (2.3) be z_2. Therefore,

$$z_1^2 = \frac{\gamma^2}{4} X - \frac{a^2 + b^2}{2} + \frac{(a^2 - b^2)^2}{4\gamma^2 X} \,, \tag{2.13}$$

$$z_2^2 = \gamma^2 z^2 + \gamma^2 \left(\frac{a+b}{2} \right)^2 \,. \tag{2.14}$$

The difference between (2.13) and (2.14) is

$$\begin{aligned}\Delta z^2 &= z_1^2 - z_2^2 \\ &= \frac{\gamma^2}{4}X - \frac{a^2+b^2}{4} + \frac{ab}{2} + \frac{(a^2-b^2)^2}{4\gamma^2 X} - \gamma^2 z^2 - \gamma^2\left(\frac{a+b}{2}\right)^2 . \end{aligned} \tag{2.15}$$

Since $\Delta z^2 \approx 2z\Delta z$, then

$$\Delta z \approx \frac{1}{2z}\left[\frac{\gamma^2}{4}X - \gamma^2 z^2 - \gamma^2\left(\frac{a+b}{2}\right)^2 + \frac{(a^2-b^2)^2}{4\gamma^2 X} - \frac{a^2+b^2}{4} + \frac{ab}{2}\right] . \tag{2.16}$$

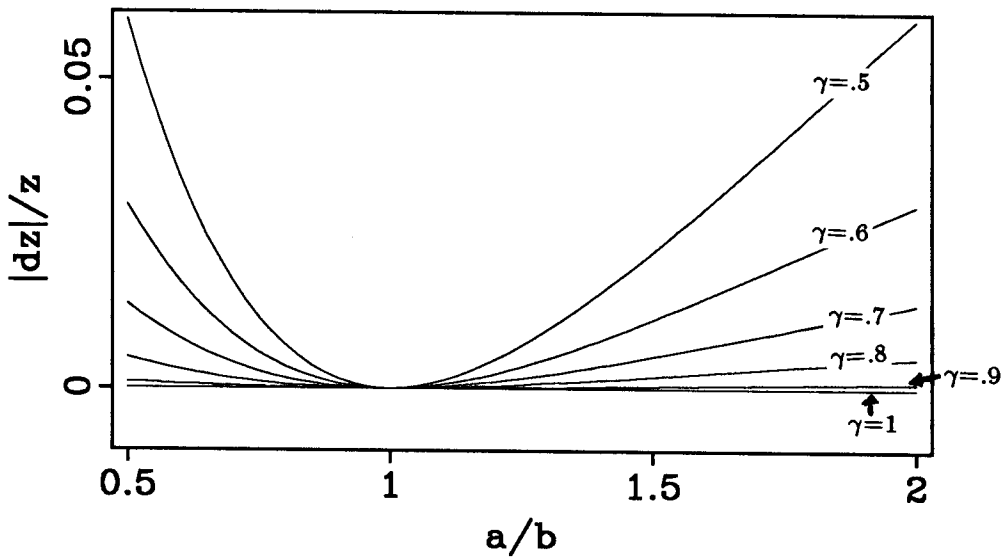

FIG. 2.14. $|\Delta z|/z$ as a function of a/b for various values of γ. Note that the error goes to zero as we approach $a = b$ for all values of γ and that it is identically zero for all values of a/b when $\gamma = 1$.

Figure 2.14 shows how $|\Delta z|/z$ varies with the ratio a/b for various values of γ. Note that the error decreases as the ratio approaches 1 and becomes identically zero when $a = b$ for all values of γ. Also, as expected, the error is always zero when $\gamma = 1$. This figure shows that the error introduced by neglecting the structure diminishes as we approach $\gamma = 1$. This means that if we start by using equation (2.3), the error estimation will not

be accurate, but after correcting the velocity model, the error estimation becomes more accurate.

2.4 OUTLINE OF THE METHOD

The discussion so far has been about average slownesses. The goal of the method presented in this thesis is to drive all images in the post-migration CRG's towards $\gamma = 1$, namely $\bar{w}_m = \bar{w}$ at all depths which means that $w_m = w$, at all depths. This goal is achieved by iteratively changing the interval-slowness model, calculating γ's, and re-migrating until the process converges. The interval slownesses are inferred from average slownesses, which are in turn calculated from γ's, and the average slownesses used in migration from equation (2.4),

$$\bar{w} = \gamma \bar{w}_m \ . \tag{2.17}$$

The velocity analysis method presented in this thesis can be summarized as follows:

- Define an initial model
- Begin loop:
  - Migrate the profiles using the current velocity model.
  - Determine γ as a function of depth by measuring the curvature in post-migration CRG's.
  - Compute average slownesses from γ and the current slowness model.
  - Compute interval slownesses from average slownesses.
  - If change in interval slownesses is small, exit loop.
- End loop.

All of the steps above have been discussed except calculating interval slownesses from average slownesses. In the next chapter, I will discuss that step in depth. Before ending this chapter, I will review some practical details that need to be considered when migrating profiles and examining CRG's.

2.5 CONVENTIONAL WISDOM

Some ideas can be borrowed from conventional processing. First, adjacent CRG's can be mixed after migration to increase signal/noise ratio (at the expense of resolution), which is similar to the mixing of adjacent common-midpoint gathers. The mixing is justified only if the subsurface has mild structure. If the structure is complicated, neighboring CRG's may be substantially different and the loss of resolution cannot be compensated by the increase in the signal/noise ratio. Second, if prestack migration is done by the hybrid method, in which time shifting is applied after downward continuation, a mute similar to NMO mute should be applied. This mute suppresses high energy introduced by excessive stretching at wide angles.

2.6 SUMMARY

In this chapter, I have shown that the image in a post-migration common-receiver gather (CRG) is aligned horizontally if the velocity used in migration is the same as the velocity of the medium. Migration with a velocity that is different from the velocity of the medium has the effect of making curved events in post-migration CRG's. I have shown the approximate quantitative relationship between the curvature and the error in the velocity model. This relationship make it possible to modify the initial velocity model. The discussion in this chapter was restricted to average slownesses. Obtaining interval slownesses from these average slownesses will be covered in the next chapter.